

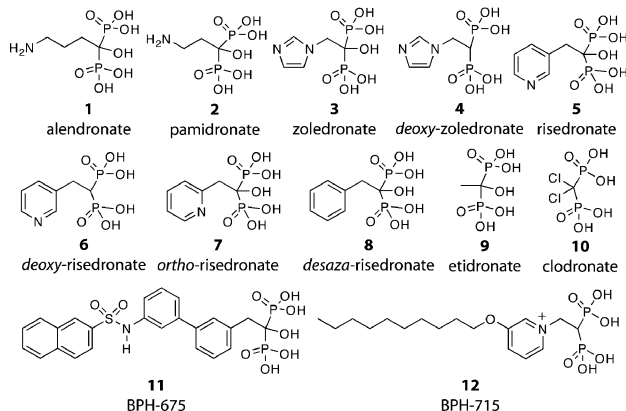
## Thermodynamics of Bisphosphonates Binding to Human Bone: A Two-Site Model

Sujoy Mukherjee,<sup>†</sup> Cancan Huang,<sup>†</sup> Francisco Guerra,<sup>†</sup> Ke Wang,<sup>‡</sup> and Eric Oldfield<sup>\*,†,‡</sup>

Center for Biophysics &amp; Computational Biology, University of Illinois at Urbana–Champaign, Urbana, Illinois 61801, and Department of Chemistry, University of Illinois at Urbana–Champaign, 600 South Mathews Avenue, Urbana, Illinois 61801

Received April 10, 2009; E-mail: eo@chad.scs.uiuc.edu

Bisphosphonates are the major drugs used to treat bone-resorption diseases.<sup>1</sup> They act by preventing osteoclastic bone resorption, inhibiting the enzyme farnesyl diphosphate synthase (FPPS). Bisphosphonates also kill tumor cells<sup>2</sup> and many parasitic protozoa<sup>3</sup> and can activate  $\gamma\delta$  T cells of the immune system<sup>4</sup> to kill tumor cells<sup>5</sup> and bacteria.<sup>6</sup> There is thus interest in their use for immuno-chemotherapy of cancer<sup>7</sup> and in the treatment of parasitic protozoan diseases,<sup>8</sup> where less avid bone binding might be advantageous. In earlier work,<sup>9</sup> we used NMR to probe how different bisphosphonates bind to bone. We found that the <sup>31</sup>P magic-angle sample-spinning NMR spectra of bound bisphosphonates exhibited a single broad peak and that there was  $\sim 0.8$  phosphate (Pi) released per bisphosphonate bound. These and other NMR results led to a model<sup>9</sup> in which a bisphosphonate  $-\text{PO}_3^{2-}$  group displaced Pi, while the cationic side chains interacted electrostatically with anionic surface groups. However, a puzzling observation was that the free energy for binding was low ( $\sim -4.3$  kcal, for pamidronate). Here, we investigate this topic further, by using isothermal titration calorimetry (ITC), which might yield information on any additional, tight binding site(s) that, if at low occupancy, would be difficult to detect via NMR.



We investigated by ITC the interaction of the 12 bisphosphonates (1–12) shown above with human bone mineral, which enabled us to study the effects of having a 1-OH group removed (4, 6), changing the position of the ring nitrogen in risedronate (7), removing the ring nitrogen in risedronate (8), and truncating the risedronate side chain (9), in addition to studying several other bisphosphonates of interest (10–12).<sup>11</sup> Representative ITC results for three compounds (1, 3, 4), together with their corresponding fitting curves, are shown in Figure 1A–B (all 12 fitting curves are

in Figure S1 in the Supporting Information, SI), and the  $\Delta G$ ,  $\Delta H$ , and  $\Delta S$  values so derived<sup>10</sup> are given in Table 1.

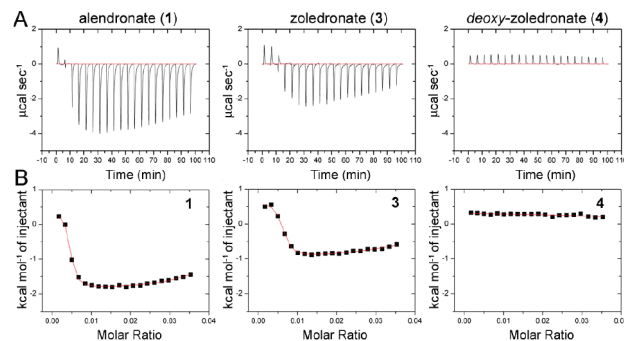


**Figure 1.** (A) ITC data for bisphosphonates 1, 3, 4 binding to human bone. (B) Representative fitting curves.

There are several observations. First, there are only two types of ITC curve seen. Binding of half of the compounds (1–3, 5, 7, and 9) is characterized by both weak (Site A, Table 1) and strong (Site B, Table 1) interactions (two independent sites), while the other six compounds (4, 6, 8, 10–12) bind to only the weak Site A (e.g., 4, in Figure 1B). Second, in most cases, binding is overwhelmingly entropy driven, that is,  $\Delta G \approx -T\Delta S$ . Third, there is a rather small range in  $\Delta S$  in both sites. In the weak binding Site A,  $\Delta G_{\text{avg}}$  is  $\sim -5.2$  kcal and  $\Delta S_{\text{avg}}$  is  $14 \text{ cal K}^{-1} \text{ mol}^{-1}$ , while in the strong binding Site B,  $\Delta G_{\text{avg}}$  is  $\sim -8.5$  kcal and  $\Delta S_{\text{avg}}$  is  $30 \text{ cal K}^{-1} \text{ mol}^{-1}$ , almost twice that seen in the weak binding site.

Based on these results, and those described previously,<sup>9</sup> we propose the bisphosphonate binding model shown (for pamidronate) in Figure 2. The weak binding Site A originates via displacement of  $\sim 1$  Pi per bisphosphonate bound. It is the one that is most highly populated (SI Table S1) and is that which is observed by NMR. One phosphonate group binds into the bone mineral matrix, and most of the binding free energy arises due to release of Pi and corresponds to a  $\Delta S$  of  $\sim 14 \text{ cal K}^{-1} \text{ mol}^{-1}$  ( $-T\Delta S_{\text{avg}} = -4.2 \text{ kcal mol}^{-1}$ ;  $\Delta G_{\text{avg}} = -5.2 \text{ kcal mol}^{-1}$ ).

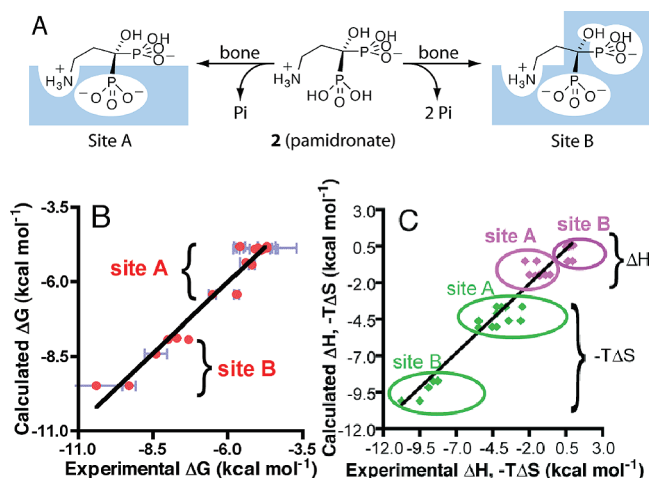
The observation that binding to the strong binding Site B is again overwhelmingly entropy driven ( $\Delta S \approx 30 \text{ cal K}^{-1} \text{ mol}^{-1}$ ,  $-T\Delta S = -9.3 \text{ kcal mol}^{-1}$ ) and that this  $\Delta S$  value is about twice that seen in the weak binding site, and that only the small 1-OH containing species bind to this site, strongly suggests the binding mode shown in Figure 2A (Site B). Here, both phosphonates (and OH) bury into the bone mineral, resulting in release of  $\sim 2\text{Pi}$  (or  $1 \text{ Pi} + 1 \text{ CO}_3^{2-}$ ) and, thus, a  $\sim 2\times$  increase in  $\Delta S$  (from  $\sim 14$  to  $\sim 30 \text{ cal K}^{-1} \text{ mol}^{-1}$ ). A 1-OH group is thus critical for bone mineral binding (as seen *in vivo*) although, interestingly, is not required for FPPS inhibition.

<sup>†</sup> Center for Biophysics & Computational Biology.

<sup>‡</sup> Department of Chemistry.

**Table 1.** Thermodynamic Parameters for Ligand Binding<sup>a</sup>

	site A <sup>b</sup>				site B <sup>c</sup>			
	$\Delta G$	$\Delta H$	$\Delta S$	$T\Delta S$	$\Delta G$	$\Delta H$	$\Delta S$	$T\Delta S$
<b>1</b>	−6.5	−1.7	15	4.7	−10.4	0.60	35	11
<b>2</b>	−5.7	−1.4	14	4.3	−9.3	0.41	31	9.8
<b>3</b>	−5.4	−1.0	14	4.4	−8.4	0.54	29	8.9
<b>4</b>	−5.2	0.49	18	5.6	−	−	−	−
<b>5</b>	−4.7	−0.69	13	4.0	−7.3	0.89	27	8.2
<b>6</b>	−4.9	0.56	18	5.4	−	−	−	−
<b>7</b>	−5.0	−1.3	12	3.7	−8.0	0.68	28	8.7
<b>8</b>	−4.8	0.86	18	5.6	−	−	−	−
<b>9</b>	−5.6	−1.4	14	4.2	−7.7	0.74	27	8.4
<b>10</b>	−5.1	−2.4	8.7	2.7	−	−	−	−
<b>11</b>	−4.7	−2.1	8.4	2.6	−	−	−	−
<b>12</b>	−5.1	−1.6	11	3.5	−	−	−	−
avg	−5.2	−0.96	14	4.2	−8.5	0.64	30	9.2

<sup>a</sup> Units of  $\Delta G$ ,  $\Delta H$ , and  $T\Delta S$  are kcal mol<sup>−1</sup>, for  $\Delta S$ , cal deg<sup>−1</sup> mol<sup>−1</sup>.<sup>b</sup> Site A is the weak binding, highly populated site. <sup>c</sup> Site B is the strong binding site.**Figure 2.** (A) Schematic of the weak (Site A, left) and strong (Site B, right) pamidronate binding sites on human bone; (B)  $\Delta G$  and (C)  $\Delta H$ ,  $-T\Delta S$  experimental versus calculated results for **1–12** binding to bone.

The results shown in Table 1 also indicate that the  $\Delta G$  for binding of alendronate (**1**) to Site B is very large (−10.4 kcal mol<sup>−1</sup>), followed by that for pamidronate (**2**; −9.3 kcal mol<sup>−1</sup>), while that for zoledronate (**3**) is less strong (−8.4 kcal mol<sup>−1</sup>) and that for risedronate (**5**, −7.3 kcal mol<sup>−1</sup>) is relatively weak. This binding strength behavior is what might be anticipated based on the  $pK_a$  values of the side chains. That is, the strongly basic species ( $pK_a \sim 11$ ) are fully protonated at pH = 7, making a strong electrostatic contribution to binding; zoledronate (imidazole  $pK_a \sim 6.7$ ) is  $\sim 33\%$  protonated, while risedronate is only weakly protonated ( $pK_a \sim 5.5$ ). In the case of the weak binding site, the  $\Delta G$  values for the OH-containing species (**3**, **5**) are only  $\sim 0.2$  kcal mol<sup>−1</sup> different from those observed with the corresponding deoxy analogues (**4**, **6**), consistent with a weak OH interaction with the surface. Of course, based on this model, it might be expected that the phenyl analogue (**8**) of risedronate (**5**) should also bind to the strong binding site. This appears not to be the case, however, presumably because the bulky phenyl group is involved in a net repulsive (anion- $\pi$ ) interaction with the bone surface. Removal of this bulky phenyl

group results in etidronate (**9**), which binds to both sites, consistent with this idea.

The question then arises: can we construct a quantitative model to predict the  $\Delta G$ ,  $\Delta H$ , and  $\Delta S$  for all 12 compounds binding into Site A and/or Site B? To do this, we used a thermodynamic group approach combined with a linear regression method, assuming that there are transferable or additive group  $\Delta G$ ,  $\Delta H$ , and  $\Delta S$  values for the cationic headgroup, each phosphonate, the 1-OH group, together with an additional term to describe the presence of a hydrophobic (1-H or phenyl) interaction. The matrix we constructed is shown in SI Table S2 and simply represents the presence (1) or absence (0) of an interaction, with the cation term (ammonium, etc.) scaled to account for  $pK_a$  differences. Four coefficients are derived from a partial least-squares analysis and are given in SI Table S3. Figure 2b,c show experimental vs predicted  $\Delta G$  (Figure 2b) and  $\Delta H$ ,  $-T\Delta S$  (Figure 2c) results, and there is good accord between experiment and prediction. For example, for  $\Delta G$ , we find the  $R^2$  value is 0.95,  $F$ -value = 88,  $p < 0.00001$ , and the error is 0.19 kcal,  $\sim 3\%$  of the overall range, using a −1.6 kcal  $\Delta G$  for binding for the  $-\text{NH}_3^+$  groups in alendronate and pamidronate, −4.8 kcal for the  $\sim -2$  charged Site A phosphonate, −3.1 kcal for the Site B phosphonate plus the OH group, and −0.05 kcal for the hydrophobic group. Good results are also obtained for  $\Delta H$ ,  $-T\Delta S$ , Figure 2c.

These results are of broad general interest since they provide the first detailed thermodynamic description of the binding of a widely used class of drug molecules, bisphosphonates, to human bone. We find the presence of two different binding sites, with binding to each being readily explained based on the structural features present in each molecule, opening the way to the design of novel, potent enzyme and cell growth inhibitors that have weak bone-binding affinity, of interest in the context of chemotherapy,<sup>11</sup> immunotherapy,<sup>7</sup> and anti-infective drug development.<sup>8</sup>

**Acknowledgment.** This work was supported by the U.S. Public Health Service (NIH Grant GM65307). S.M. was an American Heart Association, Midwest Affiliate, Predoctoral Fellow (Grant No. 0615564Z).

**Supporting Information Available:** ITC methods, data, and fitting curves for **1–12** binding to human bone, computational results, and complete ref 7. This material is available free of charge via the Internet at <http://pubs.acs.org>.

## References

- (1) Russell, R. G. *Ann. N.Y. Acad. Sci.* **2006**, *1068*, 367–401.
- (2) Green, J. R. *Oncologist* **2004**, *9* (Suppl 4), 3–13.
- (3) Martin, M. B.; Grimley, J. S.; Lewis, J. C.; Heath, H. T., III.; Bailey, B. N.; Kendrick, H.; Yardley, V.; Caldera, A.; Lira, R.; Urbina, J. A.; Moreno, S. N.; Docampo, R.; Croft, S. L.; Oldfield, E. *J. Med. Chem.* **2001**, *44*, 909–16.
- (4) Kunzmann, V.; Bauer, E.; Wilhelm, M. *N. Engl. J. Med.* **1999**, *340* (9), 737–8.
- (5) Kunzmann, V.; Bauer, E.; Feurle, J.; Weissinger, F.; Tony, H. P.; Wilhelm, M. *Blood* **2000**, *96*, 384–92.
- (6) Wang, L.; Kamath, A.; Das, H.; Li, L.; Bukowski, J. F. *J. Clin. Invest.* **2001**, *108*, 1349–57.
- (7) Gnant, M.; et al. *N. Engl. J. Med.* **2009**, *360*, 679–91.
- (8) Rodriguez, N.; Bailey, B. N.; Martin, M. B.; Oldfield, E.; Urbina, J. A.; Docampo, R. *J. Infect. Dis.* **2002**, *186*, 138–40.
- (9) Mukherjee, S.; Song, Y.; Oldfield, E. *J. Am. Chem. Soc.* **2008**, *130*, 1264–73.
- (10) Yin, F.; Cao, R.; Goddard, A.; Zhang, Y.; Oldfield, E. *J. Am. Chem. Soc.* **2006**, *128*, 3524–5.
- (11) Zhang, Y.; et al. *J. Am. Chem. Soc.* **2009**, *131*, 5153–62.

JA902895P